Is There a Change in Water Proton Density Associated with Functional Magnetic Resonance Imaging?

Thies H. Jochimsen,[1]* David G. Norris,[2] and Harald E. Möller[1]

In a recent series of studies (see, for example, Stroman et al. Magn Reson Imag 2001; 19:827–831), an increase of water proton density has been suggested to correlate with neuronal activity. Owing to the significant implications of such a mechanism for other functional experiments, the functional signal changes in humans at very short echo times were re-examined by spin-echo EPI at 3 T. The results do not confirm the previous hypothesis of a significant increase in extravascular proton density at TE = 0. Instead, an alternative explanation of the effect is offered: The use of a low threshold to identify activated voxels may generate an artificial offset in functional contrast due to the inclusion of false-positives in the analysis. Magn Reson Med 53:470–473, 2005. © 2005 Wiley-Liss, Inc.

Key words: spin-echo; fMRI; proton density; BOLD

Recently, the observation of a change in water proton density upon neuronal activation has been reported in spin-echo (SE) functional magnetic resonance imaging (fMRI) of the human brain at short echo times (TE) (1–3) and also in fMRI experiments at 0.2 T (4). It is important for the interpretation of many fMRI studies to determine whether such a mechanism exists because quantitative assessments that rely on the blood oxygenation level dependent (BOLD) contrast or on perfusion techniques would have to be corrected by this offset in fMRI signal. Therefore, SE experiments with short TE were repeated at 3 T and compared with the initial experiments as reported in Ref. (1).

MATERIALS AND METHODS

The ODIN framework (5) was used for sequence programming and data evaluation. Spin-echo fMRI experiments with varying TE were performed in an interleaved fashion to minimize the influence of intertrial variations. In addition, a third pulse is applied subsequently at each TE with a fixed mixing-time of 60 msec (Fig. 1) to acquire a stimulated echo (STE) with the same effective TE and identical sensitivity to changes in proton density, but with more diffusion/flow weighting (6,7) and a higher contribution from dynamic averaging.

After each series of different TEs, a regular SE measurement with full coverage of *k*-space, a bandwidth of 100 kHz, and TE = 80 msec is acquired as a reference to create a fixed mask of activated voxels to compute signal changes for the experiments with a variable TE.

A balanced signal-to-noise ratio (SNR) between the SE and STE experiment was achieved using flip angles of 90° for all pulses (4 msec, triangle-filtered sinc, five lobes) with the second and third pulses having a phase shift of 90° relative to the excitation pulse. The EPI readout covers 59% of *k*-space (partial Fourier) with a bandwidth of 200 kHz and TE values of 9, 19, 29, and 39 msec, and a repetition time TR = 1050 msec. Five slices (thickness 4 mm) were imaged with a field of view of 190 mm and a matrix of 64 × 64. Fat suppression by a nonselective 10-msec Gaussian-shaped pulse was applied prior to excitation. Spoiler gradients, which were used to exclude unwanted coherence pathways, introduce small diffusion/flow weighting, more pronounced in the STE experiment (b-value = 16.5 sec/mm^2) than in the SE experiment (b-value = 0.7 sec/mm^2). It has been shown (8) that the b-value of the STE experiment is sufficiently high to suppress a significant fraction of the intravascular signal.

A total of eight healthy subjects (five female, three male, 22–34 years old), who had given informed prior consent, were examined with three measurements per session on a 3-T Magnetom Trio (Siemens, Erlangen, Germany) with a birdcage head resonator. The slices were positioned to cover the visual cortex. Visual stimulation was achieved by presenting a pattern of randomly rotating L-shaped objects for 30 × TR and a period of rest with the same duration. This block was repeated 10 times per trial.

A high-pass filter with a cutoff at one quarter of the total timesteps was applied in the time domain to remove large-scale signal drifts. As in Ref. (1), spatial filtering and motion correction were omitted for the scans with a variable TE. Processing of the reference SE data with the Lipsia package (9) included a Gaussian filter (1 pixel SD) and motion correction. Activated voxels were identified by linear correlation with $p < 0.01$ and a Bonferroni correction, i.e., the significance for each voxel was set to $p' = p/N$, where N is the total number of evaluated voxels (≈8000 with a magnitude mask in our case). With this correction, the significance p' is the probability of one or more false-positives in the whole data set of one trial. These maps were then used as a mask to select the time courses of the SE and STE experiments within the same trial.

To test whether the choice of the sparse postprocessing strategy had a significant impact on the final result, the SE experiments with a variable TE were evaluated in the same way as the reference SE data. Again, the mask from the reference SE scan was then used to evaluate the time course of activated voxels.

[1]Max Planck Institute for Human Cognitive and Brain Sciences, Stephanstrasse 1a, D-04103 Leipzig, Germany.

[2]F. C. Donders Centre for Cognitive Neuroimaging, P.O. Box 9101, NL-6500 HB Nijmegen, The Netherlands.

Grant sponsor: Federal German Ministry of Education and Research (BMBF) within the framework of German-Israeli Project Cooperation (DIP).

*Correspondence to: Thies H. Jochimsen. Email: thies@jochimsen.de

Received 5 March 2004; revised 8 September 2004; accepted 9 September 2004.

DOI 10.1002/mrm.20351
Published online in Wiley InterScience (www.interscience.wiley.com).

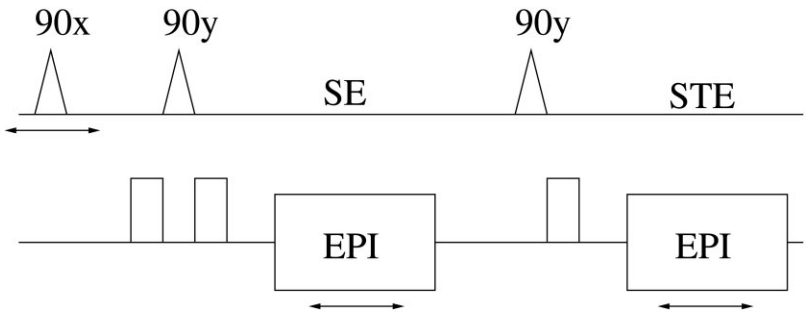

FIG. 1. Single-shot acquisition scheme for the simultaneous acquisition of spin-echo and stimulated-echo data. TE is varied by shifting the excitation pulse and the EPI-readouts on the time axis as inidicated by the arrows.

The use of a BOLD-based reference mask could be problematic if proton density changes and maximum BOLD changes occur in different voxels. To examine this possibility, maps were generated from the SE experiments with the shortest TE = 9 msec (Gaussian filter and motion correction applied) where BOLD contrast is minute. Masks, which consist of all voxels with $p < 0.005$ in a predefined region covering the visual cortex (≈1700 voxels per trial), were then used to calculate signal changes for the remaining TEs. The selected significance threshold p is just high enough so that a sufficient number of activated voxels is detected. However, in this case, an average of ≈9 voxels are expected to be false-positive in each trial.

The SE data were also evaluated with the same strategy as in Ref. (1): Individual correlation maps were calculated with $p < 0.05$ for each TE using the time courses of the data set itself rather than an independently measured data set. A region of activated voxels was then selected manually in the visual cortex, separately for each TE. The data were also inspected with a Bonferroni-corrected significance (N ≈ 1700; see above).

RESULTS

The procedure described above to identify activated voxels by an SE experiment with a fixed TE = 80 msec reveals robust functional contrast exclusively in the visual cortex of all subjects. With these masks, fMRI contrast was evaluated for the remaining experiments (Fig. 2) and fitted to a straight line, yielding the following results:

SE ($p < 0.01$, Bonferroni, reference map): $\Delta S/S_0[\%] = (26 \pm 2)$ TE/sec + (0.00 ± 0.05)

STE ($p < 0.01$, Bonferroni, reference map): $\Delta S/S_0[\%] = (21 \pm 1)$ TE/sec − (0.10 ± 0.04).

Within the accuracy of our experiments, the functional signal changes approach zero for TE → 0 in the SE experiment. In the STE experiment, a slight negative intercept is observed. However, this is an order of magnitude less than in Ref. (1). In addition, the increased sensitivity of the STE experiment to flow and diffusion decreases the fMRI contrast for all TEs.

A similar intercept is obtained for the data (not shown) that were prepared with spatial filtering and motion correction:

SE ($p < 0.01$, Bonferroni, reference map, Lipsia): $\Delta S/S_0[\%] = (22 \pm 2)$ TE/sec + (0.02 ± 0.05).

The slope of the linear fit is slightly reduced in comparison to the above result.

The results of using a mask generated at TE = 9 msec is shown in Figure 3. An average of 65 voxels was found to be activated in each trial when generating the mask. The only point deviating from a linear behavior is the one from which the mask was created. A linear fit of the remaining points yields the following results:

SE ($p < 0.005$, TE = 9 msec mask): $\Delta S/S_0[\%] = (25 \pm 1)$ TE/sec + (0.12 ± 0.02)

STE ($p < 0.005$, TE = 9 msec mask): $\Delta S/S_0[\%] = (13 \pm 1)$ TE/sec − (0.02 ± 0.02).

Again, the intercept is an order of magnitude less than in Ref (1).

However, the result is significantly different if it is derived by the same strategy as in Ref. (1), which is also depicted in Figure 2:

SE ($p < 0.05$, individual map): $\Delta S/S_0[\%] = (24 \pm 2)$ TE/sec + (0.82 ± 0.07).

With a Bonferroni correction, no activated voxels were observed at TE = 9 msec, and only a negligible number of voxels is activated at longer TEs so that a quantitative statement is impossible.

DISCUSSION AND CONCLUSIONS

The interleaved implementation of the experiments permits a nearly simultaneous measurement of fMRI contrast

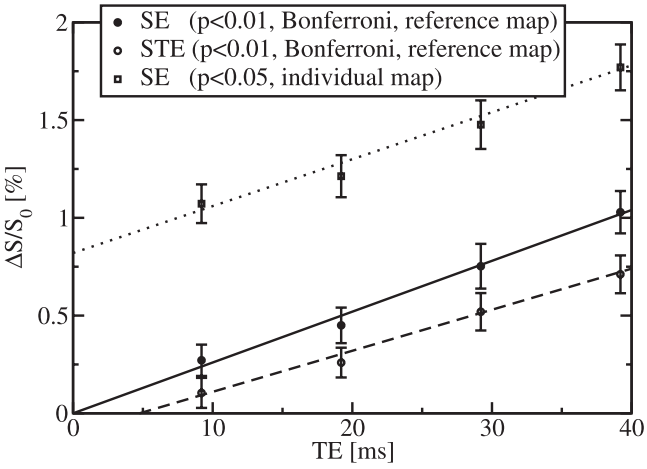

FIG. 2. Functional signal changes as a function of echo time. The values are calculated by accumulating all time courses from all trials and then subtracting the mean value of all points during activation from the mean value of all points during the resting state. The error is estimated by summing the SD of the mean value of the two states.

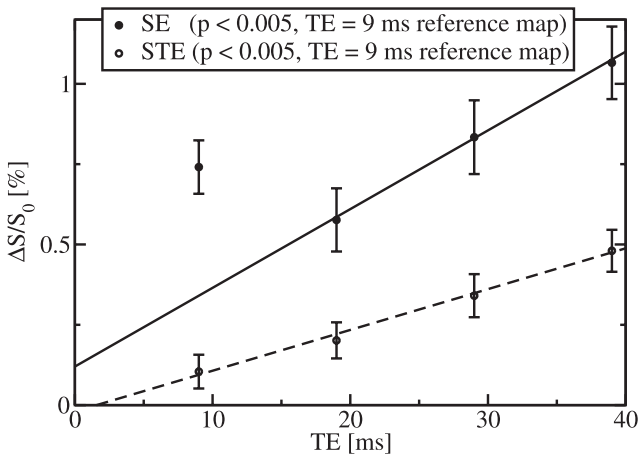

FIG. 3. Functional signal changes as a function of echo-time by using a mask generated at TE = 9 msec from the SE experiment. The point at the shortest TE was excluded in the linear fit of the SE data.

at different TEs near zero and different diffusion/flow weighting together with a reference measurement for robust determination of activated voxels. With this careful setup, a change in water proton density was not observed. Our results are consistent with the BOLD model where the functional contrast is solely based on dephasing and thus vanishes for TE = 0.

The reduced signal change in the STE acquisition, which has higher diffusion/flow weighting, confirms recent results (10) that SE-fMRI contrast at short TEs is mainly of intravascular origin at 3 T instead of extravascular dynamic averaging, which would increase fMRI contrast.

The linear coefficient for SE data presented here is in good agreement with results in Ref. (1), but the extrapolated intercept at TE = 0 differs significantly: A remaining signal change of approximately 1% at TE = 0 is not observed. The same holds for the results obtained with spatial filtering and motion correction, although the linear coefficient is slightly reduced, probably due to the blurring of pixels with large signal changes. The difference in values obtained for the intercept is probably caused by different strategies to evaluate the signal changes: By using a low threshold (large error probability) for the correlation analysis of the fMRI data, a certain number of false-positive voxels will contribute to the fMRI contrast, independent of TE. As their relative contribution increases with decreased fMRI contrast, this effect becomes more pronounced for short TEs where fMRI contrast is low. The use of an independently measured mask with a high statistical significance provides values that are not affected by this artificial effect. Consistently, no offset in fMRI signal is observed. This hypothesis is supported by the result obtained by the same strategy as in Ref. (1), which suggests a significant functional contrast at TE = 0. However, this offset is solely generated by the strategy of evaluating the fMRI data and does not reflect any physical effect. In addition, this explains that the offset was considerably less in a gradient-echo experiment in Ref. (1) because fMRI contrast is generally higher than in an SE experiment in this case. Thus, the relative number of false-positive voxels decreases. Further evidence for this explanation is the lack of activated voxels when using a Bonferroni correction, which prevents the inclusion of a significant number of false-positives.

If changes in water proton density would be located in different voxels than BOLD activation, they should at least be located within the same voxels throughout the whole range of TEs and independent of diffusion/flow weighting. In Figure 3, the point at TE = 9 msec in the SE experiment shows a high signal change, which may be independent of BOLD. However, as this is the only point in the SE experiment deviating from the usual linear behavior, and because a comparable high signal change is absent in the STE experiment at TE = 9 msec, a more plausible explanation is the contamination with false-positives: Because activated voxels are selected from the same data set that is then used to calculate fMRI signal changes at TE = 9 msec in the SE experiment, a considerable number of false-postives (estimated conservatively to be 9 of 65, as noted above) will contribute to the signal change. The remaining data points are not affected by the contamination so that they follow a linear behavior without an intercept.

There are discrepancies in the experimental setup between our study and that of Ref. (1) that could lead to different results: First, our long acquisition period using single-shot EPI in contrast to an eight-shot EPI readout leads to a higher T_2* contribution, which may generate additional fMRI contrast through a varying point-spread function (11), even at TE = 0. However, as fMRI signal change vanishes when extrapolating to TE = 0, this effect is negligible. The SNR is comparable because although the SNR per image is certainly better with an *N*-shot acquisition, the total number of images used for fMRI analysis is reduced by the factor *N*. Second, the use of a 90*x*–90*y* instead of a 90*x*–180*y* pulse sequence reduces SNR by one half, which increases the uncertainty of the percentage signal change. However, the uncertainty in our experiments is still small enough to distinguish the SE and STE experiments and to preclude a considerable change in proton density. Another consequence of a decreased SNR would be an increase in the relative contribution of false-positives when selecting activated voxels. However, this does not influence the results obtained with a reference map with strong BOLD sensitivity.

In summary, the results of this study do not provide support for the hypothesis that there is a residual fMRI contrast at TE = 0. Instead, an alternative explanation in terms of the inclusion of false-positive activation is offered. This interpretation is supported by the inability to detect an offset even when using significantly activated pixels at TE = 9 msec as a mask (c.f., Fig. 3). By using a spin-echo BOLD experiment at 3 T, it is to be expected that the BOLD activtion reported here should be well colocalized with the site of increased neuronal activity. The present study does not preclude the possibility of proton density changes located far from the site of neural activity nor does it entirely explain the ability to measure changes in proton density at very low main magnetic field strengths (4).

REFERENCES

1. Stroman PW, Krause V, Frankenstein UN, Malisza KL, Tomanek B. Spin-echo versus gradient-echo fMRI with short echo times. Magn Reson Imaging 2001;19:827–831.
2. Stroman PW, Tomanek B, Krause V, Frankenstein UN, Malisza KL. Functional magnetic resonance imaging of the human brain based on signal enhancement by extravascular protons (SEEP fMRI). Magn Reson Med 2003;49:433–439.
3. Stroman PW, Tomanek B, Malisza KL. Functional magnetic resonance imaging of the human brain and spinal cord by means of signal enhancement by extravascular protons. Conc Magn Reson A 2003;16:28–34.
4. Stroman PW, Malisza KL, Onu M. Functional magnetic resonance imaging at at 0.2 Tesla. NeuroImage 2003;20:1210–1214.
5. Jochimsen TH, von Mengershausen M. ODIN—object-oriented development interface for NMR. J Magn Reson 2004;170:67–78. URL http://od1n.sourceforge.net.
6. Song AW, Wong EC, Tan SG, Hyde JS. Diffusion weighted fMRI at 1.5 T. Magn Reson Med 1996;35:155–158.
7. Boxerman JL, Bandettini PA, Kwong KK, Baker JR, Davis TL, Rosen BR, Weisskoff RM. The intravascular contribution to fMRI signal change: Monte Carlo modeling and diffusion-weighted studies in vivo. Magn Reson Med 1995;34:4–10.
8. Jochimsen TH, Norris DG, Mildner T, Möller HE. Quantifying the intra- and extravascular contributions to spin-echo fMRI at 3 Tesla. Magn Reson Med 2004;52:724–732.
9. Lohmann G, Müller K, Bosch V, Mentzel H, Hessler S, Chen L, Zysset S, von Cramon DY. Lipsia - a new software system for the evaluation of functional magnetic resonance images of the human brain. Comp Med Imag Graph 2001;25:449–457.
10. Duong TQ, Yacoub E, Adriany G, Hu X, Ugurbil K, Kim SG. Microvasculatur BOLD contribution at 4 and 7 T in the human brain: gradient-echo and spin-echo fMRI with suppression of blood effects. Magn Reson Med 2003;49:1019–1027.
11. Birn R, Bandettini P. The effect of T2′ changes on spin-echo EPI-derived brain activation maps. Proc Intl Soc Mag Reson Med 2000; 10:1324.